EFDA–JET–CP(10)06/03

V. Riccardo, G. Arnoux, P. Cahyna, T.C. Hender, A. Huber, S. Jachmich,
V. Kiptily, R. Koslowski, L. Krlin, M. Lehnen, A. Loarte, E. Nardon,
R. Paprok, D. Tskhakaya and JET EFDA contributors

JET Disruption Studies in Support of ITER

"This document is intended for publication in the open literature. It is made available on the understanding that it may not be further circulated and extracts or references may not be published prior to publication of the original when applicable, or without the consent of the Publications Officer, EFDA, Culham Science Centre, Abingdon, Oxon, OX14 3DB, UK."

"Enquiries about Copyright and reproduction should be addressed to the Publications Officer, EFDA, Culham Science Centre, Abingdon, Oxon, OX14 3DB, UK."

The contents of this preprint and all other JET EFDA Preprints and Conference Papers are available to view online free at www.iop.org/Jet. This site has full search facilities and e-mail alert options. The diagrams contained within the PDFs on this site are hyperlinked from the year 1996 onwards.

JET Disruption Studies in Support of ITER

V. Riccardo[1] , G. Arnoux[1], P. Cahyna[2], T.C. Hender[1], A. Huber[3], S. Jachmich[4], V. Kiptily[1], R. Koslowski[3], L. Krlin[2], M. Lehnen[3], A. Loarte[5], E. Nardon[1], R. Paprok[6], D. Tskhakaya[7] and JET EFDA contributors*

JET-EFDA, Culham Science Centre, OX14 3DB, Abingdon, UK

[1]EURATOM/CCFE Fusion Association, Culham Science Centre, Abingdon, OX14 3DB, UK
[2]Institute of Plasma Physics, Association EURATOM/IPP.CR, Prague, Czech Republic
[3]Institute Energieforschung-4, Forschungszentrum Jülich, EURATOM- Association, Jülich, Germany
[4]LPP-ERM/KMS, EURATOM-Belgian State Association, TEC, Brussels, Belgium
[5]ITER Organization, Cadarache, France
[6]Charles University Prague, Faculty of Mathematics and Physics, Prague, Czech Republic
[7]Association EUROATOM, Institute of Theoretical Physics, Innsbruck University, Austria.
** See annex of F. Romanelli et al, "Overview of JET Results",*
(Proc. 22 [nd] IAEA Fusion Energy Conference, Geneva, Switzerland (2008)).

Preprint of Paper to be submitted for publication in Proceedings of the
37th EPS Conference on Plasma Physics, Dublin, Ireland.
(21st June 2010 - 25th June 2010)

ABSTRACT.
Plasma disruptions affect plasma facing and structural components of tokamaks due to electromechanical forces, thermal loads and generation of high energy runaway electrons. Asymmetries in poloidal halo and toroidal plasma current can now be routinely measured in four positions 90o apart. Their assessment is used to validate the design of the ITER vessel support system and its in-vessel components. The challenge of disruption thermal loads comes from both the short duration over which a large energy has to be lost and the potential for asymmetries. The focus of this paper will be on localised heat loads. Resonant magnetic perturbations failed to reduce the generation of runaway electrons in JET. An explanation of the limitations applying to these attempts is offered together with a minimum guideline. The REs generated by a moderate, but fast, Ar injection in limiter plasmas show evidence of milder and more efficient losses due to the high Ar background density.

1. INTRODUCTION

The ITER design and the need to ensure its integrity over several years of operation guide the scope of disruption studies in present tokamaks. JET can contribute to the understanding of asymmetric Vertical Displacement Events (VDE), Section 2, the assessment of localised heat loads, Section 3, and in the study of Runaway Electrons (RE) and of ways to control them, Section 4.

2. ELECTROMECHANICAL LOADS

Disruptions cause electromechanical loads in two ways: induced current due to fast varying magnetic fields from the plasma current decay and movement and current with a composite path, partially in the edge of the plasma and partially flowing in the plasma facing conductive structures and the vessel wall (halo current). Electromechanical loads have been a driver in the design of ITER plasma facing components, vessel and its supporting structure. For most of these the achievable margin is small and most of the uncertainty is in the input loads.

JET has contributed the current quench data to the International Disruption Database [1]. At that time the JET the lower bound of the current decay time normalised to the plasma cross-section area before the disruption was larger than ~3 ms/m2. However, following the installation and feedforward use of the Disruption Mitigation Valve (DMV) [2], faster current quenches have been observed, especially after the injection of pure Ar and Ne. With the caveat that the linear current decay time had to be extrapolated from interval covering 100% to 70% of the plasma current decay to avoid any influence from the runaway current plateau (instead of 80% to 20% as in the IDDB), the fastest normalised current decay has been found at ~1.4 ms/m^2 for pure Ar below 1.7 ms/m^2, the minimum quench time established from all tokamaks in the IDDB.

2.1. HALO AND PLASMA CURRENT ASYMMETRIES

In the 2004–2005 shutdown, four arrays of halo current diagnostics have been installed behind the tiles of the upper dump plate (a ~800mm arched ring of 8 rows of tiles) in four octants, at $\phi = 0, \pi/2, \pi$ and $3\pi/2$ [3]. Each array comprises 1 to 2 toroidal field pick-up coils and up to eight Rogowskii coils, behind each tile representative of a toroidal row of tiles.

The Rogowskii coils became operational only after the 2007 shutdown. Soon it was confirmed that the current density they measure is consistent with the total poloidal halo current measured by the toroidal field pick up coils. During upward events the Rogowskii coils showed that the halo footprint extends over most of the dump plate, the same region of the dump plates as the heat flux measured by the IR camera. From this the halo flux tube width is estimated 100mm at the time of the peak poloidal halo current.

The availability of four toroidally evenly spaced measurements of the poloidal halo current allows the asymmetry in the plasma to be compared with the asymmetry of the poloidal halo current. This was a crucial piece of information missing in the initial analysis of the JET asymmetric VDEs [4-6]. When the edge safety factor becomes sufficiently small during a VDE, the plasma current and vertical current moment are n = 1 toroidally asymmetric. These asymmetries can lead to substantial sideways forces in JET, observed up to ~4MN, and are expected to be an order of magnitude larger in ITER, designed for 48MN. In addition, while in JET the mechanical response of the vessel is on time scales much longer than the duration of the disruption and the worst loading case is determined by the impulse of locked asymmetries, in ITER the vessel mechanical response time could be shorter than the duration of the longest expected VDEs, so also rotating modes resonating with the vessel are of concern as this could lead to a strong enhancement of the vessel distortions.

The ITER asymmetric forces are estimated using the source and sink model [6] for which the input needed is the amplitude of the plasma current asymmetry, its duration and its rotational frequency, if any. The assessment of 7 JET asymmetric VDEs [7] suggested the worst case can be covered by 10% of the pre-disruption current lasting 37.5ms (in JET). This assessment has been revisited [8] now that fast sampling rate is routinely available for the magnetic measurements in four octants. The integral of the asymmetry amplitude can be as large as an average of 10% for the whole duration of the current quench for short to moderate current quench durations (up to 50ms) and it is significantly lower for the longest events. If the asymmetry characteristics can be ported to ITER, this means that only events shorter than 250ms will have large asymmetries. If these rotate at low frequencies, which are of concern for the ITER vessel, these will complete only very few rotations limiting the force amplification factor.

Recently the assessment of asymmetric VDE has been expanded to investigate not only locked but also rotating events. The rotation frequency is mainly between 50 and 150Hz in direction opposite to the plasma current. However, frequencies have been observed as high as 280Hz and negative (co-plasma) as large as 200Hz. Of the events with significant asymmetry (and with available data) less than 20% rotate in the same direction as the plasma current. The frequency seems to be independent from the amount of asymmetry of the event. The physics processes leading to these rotation variations are not presently clear. A striking example of a rotating asymmetry is shown in Figure 1. The poloidal halo current is measured using toroidal field pick up coils, therefore this is the axis-symmetric extrapolation from the field variation in/near the location of the probe. The asymmetry starts at the very beginning of the current quench. By this time the plasma has already moved >75cm upwards, nearly reaching the position where it will spend the rest of the disruption. The last converged solution of the magnetic reconstruction is a t=27.95s, when the plasma has moved

~70 cm, and has the edge safety factor equal to 1.1. The asymmetry disappears when the plasma current has decreased below 20% of the pre-disruption value. The bottom four boxes of Figure 1 show the asymmetric component of the poloidal halo current and the toroidal plasma current in each octant. This is defined by taking away the current averaged over the four octants from the current in each octant. Once the asymmetry is established, in this case, its amplitude stays nearly constant throughout the event and rotates at nearly constant frequency, ~280Hz. The amplitude does not always stay constant during the event and the rotation is rarely this clear, in some cases locked and rotating periods are present, whilst there is usually a good correlation between the phase and the amplitude of the halo and plasma asymmetry. The asymmetric component of the plasma current has been deliberately plotted $\pi/2$ ahead of that of the halo current to emphasise the phase shift between halo and plasma, and also allow a comparison between the amplitudes, which are nearly identical. Along the direction of flow of the plasma current, the asymmetric component of vessel current, which has to be approximately the opposite of the plasma current asymmetric component (~cosϕ), peaks $\pi/2$ after the halo current asymmetry (~sinϕ), as if the vessel current was the integral of the halo current asymmetry. Assuming $n = 1$, the integral of the halo asymmetry over the half torus providing the current source is $2\delta_{h0}$, with $2\delta_{h0}$ the amplitude of the halo asymmetry, while the step in plasma current between the end points of the integration interval $-2\delta I_{p0}$, where δI_{p0} is the amplitude of the plasma current asymmetry. For these to be equal $2\delta_{h0} = 2\delta_{p0}$. The amplitude of the two asymmetries correlates well also over relatively long intervals, for example as the integral over the longest time interval when the plasma current asymmetry amplitude is above an appropriate threshold.

3. THERMAL LOADS

During JET plasma disruptions, the thermal energy (<12MJ) and magnetic energy (<60MJ) are lost in form of heat to the plasma-facing components on timescales of ~1ms and >20ms respectively [9]. In ITER the thermal energy (<350MJ) and the poloidal magnetic energy (<1300MJ) are over an order of magnitude larger than in JET [10]. JET might run close to the material limits when the new all-metal wall is installed (with melting at ~20MW/m^2 s$^{1/2}$ for Be and at ~50MW/m^2 s$^{1/2}$ for W), therefore there is a greater concern for the plasma facing components life time. The challenge comes from both the short duration over which a large energy has to be lost and the potential for asymmetries.

3.1. THERMAL LOADS FOLLOWING THERMAL QUENCH AND DURING THE CURRENT QUENCH

Fast IR and bolometric [11] data have been collected during discharges ending in four types of planned natural disruptions at high plasma stored energy: density limit [12], radiative collapse [12], low-q static X-point [13] and upward VDE. Only the latter is discussed here in detail.

Three high-triangularity, high-bp (~2.5MJ thermal stored energy), 1.5MA plasmas have been pushed upwards using the vertical control system. The two with the best diagnostics available are plotted in Figure 2. The plasma position dynamics is very similar in the two cases. The offset time of the thermal quench is ~0.031s for both. The energy collected by the dump plate is the same in the two cases, ~1.2MJ, but the time behaviour and the peak power density are different. In one case the

load, at least at the observed toroidal position, is more evenly distributed poloidally and smoother in time than in the other case. The dump plate heat flux shows a thermal quench component followed by a current quench component. The total radiated power is rather different in the two cases. One could speculate that in the event where the interaction with the dump plate was more localised (in time and space) more impurities were injected enhancing the radiation.

The inspection of these VDEs highlights the uncertainties due to peaking factors. In JET only one toroidal position was viewed with IR, while there is a horizontal and a vertical bolometer in different toroidal positions, however axis-symmetry needs to be assumed for their interpretation. Therefore in JET toroidal peaking factors in the heat loads cannot be assessed. Instead radiation poloidal peaking factor (RPPF = peak / average) has been analysed [11] showing that VDEs have the largest asymmetries. Density limit, radiative collapse and low-q disruptions have ~2.5, while VDEs have up to 3.5 RPPF. In VDEs the radiation distribution is mostly located in the vicinity of the upper dump plate. This strongly localised radiation is most likely the result of an increased local impurity influx to the main chamber plasma which can, in addition to the convective heat loads, lead to significant local radiation loads. In a combined VDE+DMV disruption, plotted in Figure 3 the cooling phase started ~10ms after the VDE had been triggered and when the plasma had displaced ~20cm. As a result of the cooling the vertical velocity is temporarily increased until the thermal quench occurs when the plasma has only moved ~40cm in total (much less than in a normal VDE, ~80cm). In this case the RPPF is 2.14 at the thermal quench instead of 3.33 of the reference VDE. This reduction could be simply because the plasma was made to disrupt before getting as close as usual in a VDE to the dump plate. The RPPF after DMV injection peaks as the gas starts interacting with the plasma, at this time though the lost energy is small and so the local power density. The pre-thermal quench energy loss associated with the use of the DMV helps reducing the peak power density at the thermal quench as well. In fact, in the case shown in Figure 3 the peak power density is for VDE+DMV is 1.76MW/m^2 while for pure VDE is 3.28MW/m^2, less than proportional to the ratio of RPPFs.

3.2 THERMAL LOADS DUE TO RUNAWAY ELECTRONS

In ITER RE currents are predicted up to 10MA, 70% of the pre-disruption current, with an energy content of 20MJ if confined until q = 2 is reached at the edge, and an average energy of 12.5MeV [14]. This is far larger than in JET: typically 1MA (50% of 2MA, although historically 2.5MA from 6MA events have been observed) and 0.5MJ with average energy 10MeV. Therefore the danger posed by RE in JET is modest compared to ITER, but the effect significant enough to be observable and contribute to a refinement of the understanding of the loads associated with the RE loss to the wall.

In a large set of pure Ar and pure Ne DMV triggered disruptions of ohmic X-point plasmas, 17 caused distinctive localised heating of the upper dump plate in 5 spots within the view of the IR camera. The location of the 5 point is driven by the installation variation of the tiles rather than plasma asymmetries. Four of the hot spots appear on the same row of dump plate tiles, the fifth on the next row. This suggests the interaction region is ~1.3m^2. The collection area is significantly smaller due to the unevenness of the dump plate. Assuming the pattern observed in the viewed octant continues,

the wetted area is 0.3-0.5m^2. Typically the temperature at these spots rises first at the thermal and then when the RE are lost, i.e. when the SXR signals collapses and the plasma current restarts to decay [13]. The second peak is larger than the first in these 17 disruptions. For these the RE current has been estimated as the maximum departure from the exponential decay with the decay time evaluated in the first 3 ms of current decay and the RE energy from the integral of the loop voltage. The RE beam energy is plotted in Figure 4 with the average temperature increase of the hot spots. The extent of the temperature error bars cover minimum to maximum temperature increase, while the energy is the average between the one obtained stopping the loop voltage integral either at the beginning or at the end of the RE current drop. Within the uncertainty of the average electron energy and the depth of the heat deposition, the RE beam energy is consistent with the observed temperature increase. For example 0.5MJ correspond to 800^{o}C surface temperature increase, which over ~2ms requires the loss to occur on 0.5m^2, consistent with the observed hot spots.

4. RUNAWAY ELECTRONS

Having looked at the effects of RE on the wall, here we discuss ways of dealing with RE other than by massive gas injection, which is discussed in [2] for JET and in [15-19] for other tokamaks.

4.1 RESONANT MAGNETIC PERTURBATION

Resonant Magnetic Perturbation (RMP) is an attractive alternative to massive gas injection to suppress RE as it is less demanding for the plant. This technique has been explored in JT-60U [20] and TEXTOR [21] disruption generated RE, showing that runaways are absent for a sufficient high perturbation field.

In fact, electrons undergo radial transport due to magnetic fluctuations, which reduces the avalanche growth rate since the RE leaving the plasma do not produce any new ones in close collisions with thermal electrons [22]. Even if avalanche cannot be prevented, its growth rate can be sufficiently reduced so that there is not enough flux to achieve significant growth. The field perturbation to achieve this is $\delta B/B \sim 10^{-3}$. In JET external perturbation fields can be applied using the Error Field Correction Coils (EFFC). The system consists of four square shaped coils (6m in dimension) which are mounted at equally spaced toroidal positions and attached to the transformer limbs [23]. Each coil spans a toroidal angle of 70^o and has a radial distance along the winding of 5.3–7m from the axis of the machine. It has so far being operated up to a maximum current per coil of 48kAt. These coils can be set up to produce either $n = 1$ or $n = 2$ fields. Both modes have been applied to disruptions which reliably produce RE in JET over a range of plasma current and toroidal field combinations at constant edge safety factor. The most analysed combination is $I_p = 1.7$MA and $B_t = 2.7$ T with one pair of coils in $n = 1$ (hardware driven limitation) at 2kA $\times$ 16 runs applied before and during the disruption to ensure vessel penetration, while plasma penetration is assumed being the plasma cold, especially after the disruption (a few eV). Generally the application of EFCC shows no effect on RE generation in JET. The effective resonant magnetic perturbation scaled form [24] for the combination of applied toroidal field and EFCC current is $1.7\ 10^{-4}$ at $q = 2$ and $1.3\ 10^{-4}$ at $q = 3$, so lower than necessary according to [22]. Assuming a parabolic profile for

the plasma current density, the island width and their overlap can be estimated. All the islands are small (<0.1 $\varphi_{norm}^{1/2}$), as is their overlap expressed as Chirikov parameter: the overlap between m = 2/n = 1 and m = 3/n = 1 is $\sigma_{Chir}^{2,3} \sim 0.61$ and between m = 3/n = 1 and m = 4/n = 1 is $\sigma_{Chir}^{3,4} \sim 0.54$. This suggests little interaction between the islands and it is confirmed by numerical investigation of the motion of charged particles in perturbed magnetic fields, taking into account orbit shifts for 5-10-20MeV electrons [25] and using both a parabolic profile and a significantly more peaked one to account for the RE being mainly in the centre of the plasma. Drift relativistic Hamiltonian is used [26] and its accuracy confirmed by a sample comparison with a full Larmor Hamiltonian and by checking energy conservation. Speculative calculations with higher EFCC current (6kA × 16 turns in two n = 1 pairs) show that even this level of perturbation might be insufficient, as ergodization only appears when the most peaked profile is used and there only on the outer surfaces leaving the centre, and so the RE, well confined.

Also the modulation of the Toroidal Tield (TF) due to the finite number of TF coils deteriorates the confinement of the electrons [27]. If the electron cyclotron motion is in resonance with the modulation frequency the electrons are scattered in pitch angle, increasing the power radiated per electron. A resonance occurs at $\gamma = (eB_tR)/(nNm_ec)$, where n is the mode number and N is the TF ripple mode number, for typical JET planned RE disruptions this corresponds to ~120/n MeV TF ripple driven RE energy limit. For low mode numbers this is much higher than the synchrotron energy limit (20MeV for minimum pitch angle) and the energy limit set by the flux (~30MeV if $\int V_{loop}\, dt \sim$ 1.5Vs), while the strength of the resonance decreases with increasing mode number. This is too high energy to be of interest for JET. However, if the ripple strength is sufficiently high ($\delta B/B > 1/(nNq)^2$, where q is the boundary safety factor), neighbouring poloidal harmonics should overlap [27], providing additional pitch angle scattering. The threshold condition for this to occur is ~$2.4\ 10^{-4}$ for typical JET planned RE and N = 16. At the time RE are present only the inner side of the plasma for normalised radius >0.5 satisfies this condition. This makes the TF ripple an unlikely tool to limit RE generation, as confirmed in a set of four TF ripple shots and by full Hamiltonian calculations following 5-10-20MeV electrons both for parabolic and peaked current profiles.

4.2 HIGH BACKGROUND DENSITY

The plant has been kept active in presence of disruption REs to test mitigation techniques. The removal of ohmic support has been proven inefficient as the plant does not allow the voltage applied to the central solenoid to be reversed and the RE beam resistance is low so consuming very little flux. The injection of gas after the RE disruption was triggered using the DMV also has been proven inefficient as the amount of Ar atoms injected by the normal injection system (~1.5×10^{21}) is far smaller than that already injected by the DMV (6×10^{22}).

The features of RE triggered by low pressure Ar DMV injection on limiter plasmas are significantly different from those of either natural or radiative collapse triggered RE. The first apparent difference is that the RE tail current in DMV-triggered events rather than staying constant until the RE beam is lost due to either vertical or internal instability drops at 7.5 MA/s for ~6×10^{22} injected Ar atoms, Pulse No: 79427 in Figure 5. The current decay rate is not significantly affected when the number

of injected Ar is increase in steps to ~13×10^{22}; the tail is too short to assess at 21 1022 Ar and at 6×10^{22} Ne. The photoneutron count is much larger when the DMV is used as a trigger, but the heat loads are similar to that of a radiative collapse driven event: for the pair Pulse No's: 79424-79427 the same energy is collected on the inner and outer walls; whilst the short term temperature increase is much larger on the dump plate for the DMV as the plasma has moved further up, the long term is identical. Having aligned the time of the quench in Figure 5 it is apparent that RE generation starts earlier in the DMV triggered event. The ratio HXR/γ is on a downward trend for the radiative collapse event showing a decay in the average energy content of the population, whilst in the DMV event the average energy content first increases slowly and then it remains constant whilst the current decays gently, consistent with HXR energy spectra. 2-D tomographic reconstruction carried out during disruptions using a new method based on the detection of Compton scattering [28] of emission fast electron bremsstrahlung confirm that the energy is kept nearly constant during the current tail and also show that the peak HXR emission comes from the plasma region rather than the wall. In addition, substantial radiation is observed during DMV triggered RE current tails, while in natural RE current tails radiation is negligible. These observations indicate that the electrons are interacting with the background Ar density.

During the steady decay the plasma time constant is tIp~0.23 s and the avalanche growth time is ts~0.08 s. For these to be consistent, -1/tIp=1/ts-1/tloss, tloss needs to be ~0.06 s. From the electron stopping time in Ar [29], the required loss time can be estimated as ~0.5 1020 m-3, which is less than the average Ar density in the JET volume 140 m3 when 6 1022 Ar atoms are injected (but not necessarily penetrated).

CONCLUSION

Substantial progress has been made in quantifying disruption consequences, leading to an improved physics basis for ITER.

- The poloidal halo current asymmetry has nearly the same amplitude as the toroidal plasma current asymmetry in VDEs. The asymmetries rotate together with a 90^{o} lag between them, typically counter-plasma. The amplitude of the current asymmetry (responsible for the ITER sideways force) averaged over the current quench duration is <10% the pre-disruption plasma current. The 10% envelope is approached only up to current quench times of 50ms, so large asymmetries can only complete a small number of revolutions at low frequencies.
- The most poloidally localised heat loads have been observed in VDEs, both by IR and by bolometry. Radiation poloidal peaking factors up to 3.5 have been recorded in VDEs, these are reduced by DMV.
- RE heat loads relate to the RE current and non-magnetic energy. The total area of interaction is relatively large (~1.5 m^2) but the area actually wetted is smaller, in the JET case due to installation tolerances.
- High Ar density background, torus average ~4×10^{20} m^{-3}, achievable with the DMV, leads to a gentle loss of RE population, minimising the residual stored energy to be suddenly lost to the wall.

ACKNOWLEDGEMENTS

Work conducted under EFDA and partly funded by the UK EPSRC under grant EP/G003955 and the EC under the contract of Association between EURATOM and CCFE. The views and opinions expressed herein do not necessarily reflect those of the European Commission.

REFERENCES

[1]. J. Wesley *et al*., Disruption Characterization and Database Activities for ITER, Proc. 21st IAEA Fusion Energy Conf., Chengdu, China, 2006

[2]. M. Lehnen *et al*.., First Experiments on Massive Gas Injection at JET - Consequences for Disruption Mitigation in JET and ITER, Proc. 36th EPS Conf. on Plasma Physics, Sofia, Bulgaria, 2009

[3]. V. Riccardo *et al*., Nuclear Fusion **49** (2009) 055012

[4]. P. Noll *et al*., Proc. 19th SOFT on Fusion Technology (16–20 September 1996, Lisbon)

[5]. V. Riccardo *et al*., Fusion Engineering Design **47** (2000) 389–402

[6]. V. Riccardo *et al*., Nuclear Fusion **40** (2000) 1805–10

[7]. C. Bachmann, Asymmetric Forces on the ITER Vacuum Vessel due to the Sink and Source Model, ITER_D_2DJ5AA v2.7

[8]. S. Gerasimov, Scaling JET disruption sideways forces to ITER, Proc. 37th EPS Conf. on Plasma Physics, Dublin, Ireland, 2010

[9]. V. Riccardo *et al*., Nuclear Fusion **45** (2005) 1427

[10]. A. Loarte *et al*., Physics Scripta **T128** (2007) 222–228

[11]. A. Huber *et al*., Radiation loads onto plasma-facing components of JET during transient events - experimental results and implications, PSI 2010, Proc. 19th International Conf. on Plasma

[12]. G. Arnoux *et al*., Nuclear Fusion **49** (2009) 085038.

[13]. G. Arnoux *et al*., Heat Load Measurements on the JET First Wall during Disruptions, PSI 2010, Proc. 19th International Conf. on Plasma Surface Interactions, San Diego, Ca, USA, 2010 Surface Interactions, San Diego, Ca, USA, 2010

[14]. T. Hender *et al*., Nuclear Fusion **47** (2007) S128–S202

[15]. G. Pautasso *et al*., Plasma Physics and Controlled Fusion **51** (2009) 124056

[16]. C. Reux *et al*., Experimental study of gas jet dynamics during disruption mitigation using massive noble gases injections on Tore Supra, Proc. 36th EPS Conf. on Plasma Physics, Sofia, Bulgaria, 2009

[17]. S. Bozhenkov et al., Efficiency of massive gas injection for increase of plasma density in TEXTOR experiments on disruption mitigation, Proc. 36th EPS Conf. on Plasma Physics, Sofia, Bulgaria, 2009

[18]. D. Whyte et al., Jour Nucl Mat **363-365** (2007) 1160-1167

[19]. E. Hollmann *et al*., Nuclear Fusion **48** (2008) 115007

[20]. R. Yoshino *et al*., Nuclear Fusion **40** (2000) 1293

[21]. M. Lehnen *et al*., Physical Review Letters **100** (2008) 255003

[22]. P. Helander *et al.*, Physics of Plasmas **7** (2000) 4106
[23]. I. Barlow *et al.*, Fusion Engineering Desing **58-59** (2001) 189 - 193
[24]. Y. Liang *et al.*, Plasma Physics and Controlled Fusion **49** (2007) B581
[25]. R. Paprok *et al.*, Motion of charged particles in perturbed fields in tokamak, WDS09 Proc Contrib – Part II (2009) 139-143
[26]. A. Wingen *et al.*, Nuclear Fusion **46** (2006) 941
[27]. J.M. Rax *et al.*, Runaway dynamics in Tokamaks, New ideas in Tokamak confinement (1992) 154
[28]. G.F. Knoll, Radiation detection and Measurement, New York, Wiley & Sons, 1989
[29]. http://physics.nist.gov/Star, National Institute of Standards and Technology, Gaithersburg, MD, USA

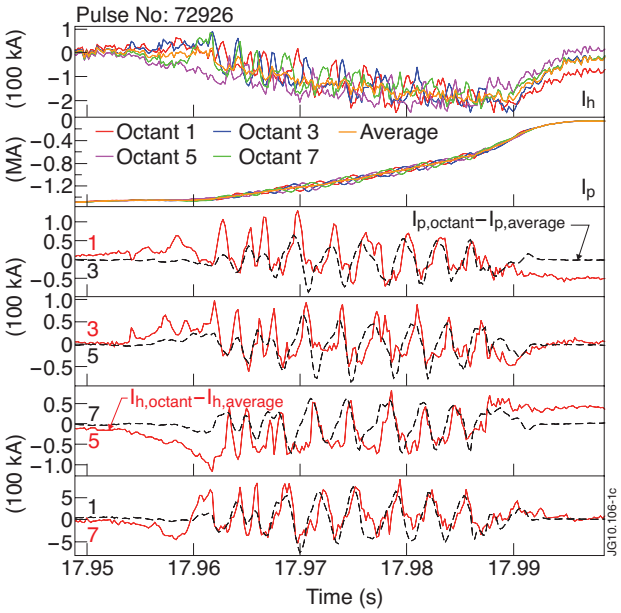

Figure 1: The poloidal halo current and the plasma current measured in four octants are in the top two boxes. The plasma current flows clockwise in JET, hence the negative sign. Negative halo current in the top of the vessel means current entering outboard and exiting inboard. The bottom four boxes have the asymmetric component of the poloidal halo current and the asymmetric component of the toroidal plasma current in each octant, with the plasma shifted toroidally by π/2.

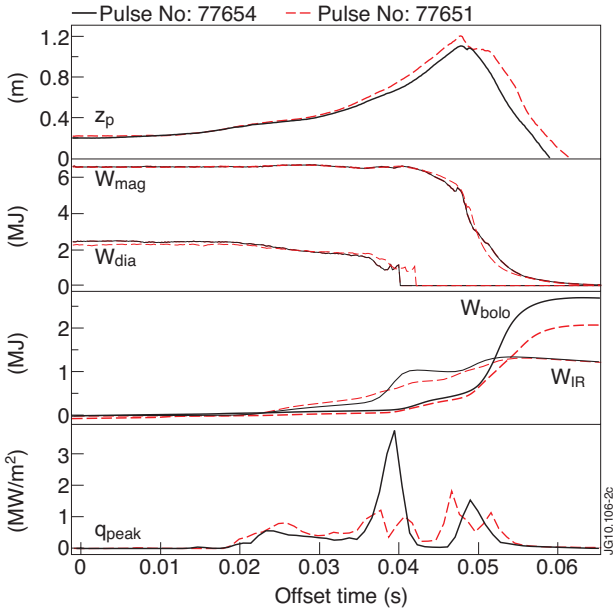

Figure 2: Plasma vertical position, thermal stored energy (W_{dia}) and magnetic energy (W_{mag}), radiated energy (W_{bolo}, measured by bolometry) and energy collected by the upper dump plate (W_{IR}, measured by IR) both zeroed close to the time of the kick, peak power density on the upper dump plate for two planned VDEs.

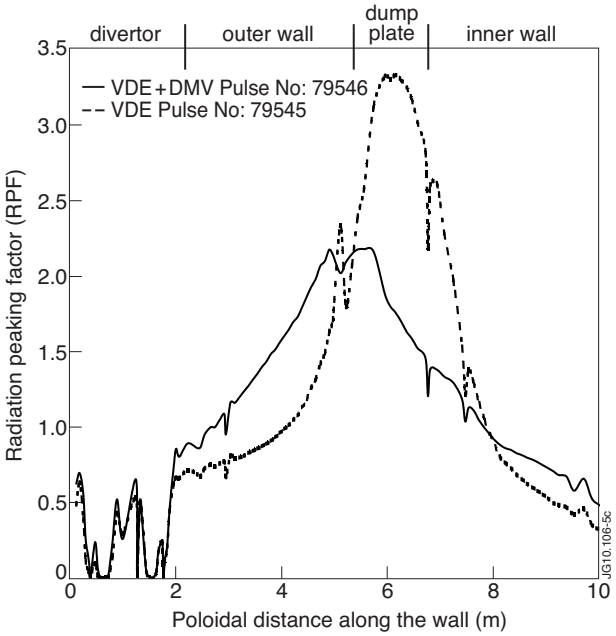

Figure 3: RPPF at the thermal quench for a pure VDE and a VDE interrupted by the DMV, both with about 2.8 MJ stored plasma energy.

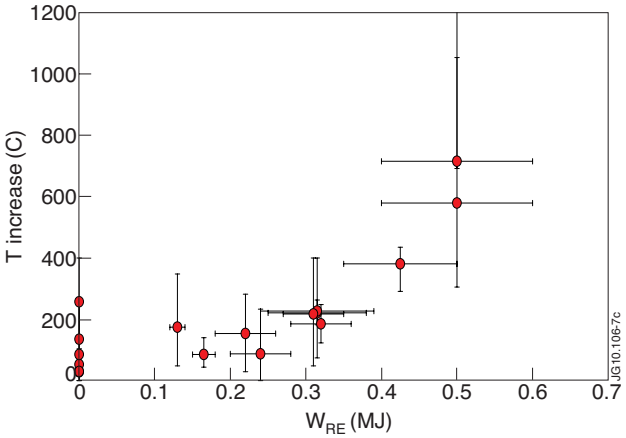

Figure 4: Non-magnetic RE energy plotted versus the average hot spot temperature increase.

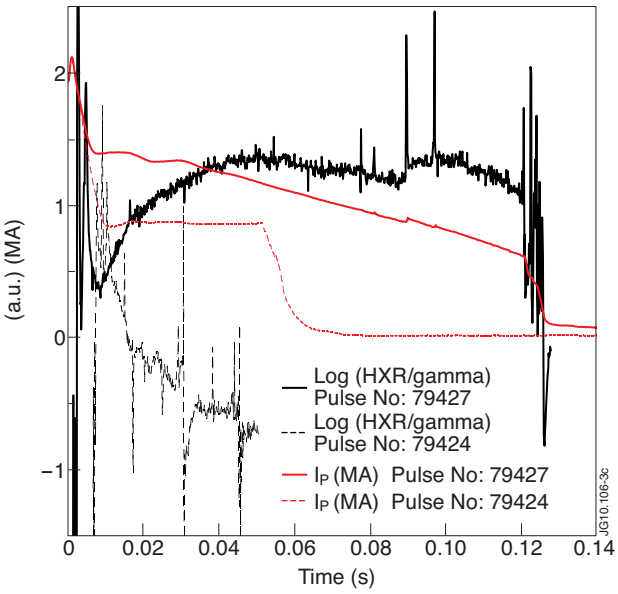

Figure 5: Plasma current and ratio of HXR to γ-ray counts for two RE events: Pulse No: 79424 caused by a radiative collapse and Pulse No: 79427 DMV triggered.